



Journal Homepage: - www.journalijar.com

INTERNATIONAL JOURNAL OF ADVANCED RESEARCH (IJAR)

Article DOI: 10.21474/IJAR01/13167

DOI URL: <http://dx.doi.org/10.21474/IJAR01/13167>



RESEARCH ARTICLE

TENOXCAM PERFORMANCES FOR ALUMINIUM CORROSION INHIBITION IN 2M H₂SO₄: EXPERIMENTAL AND QUANTUM CHEMICAL APPROACHES

Kalifa Mariko¹, Donourou Diabaté² and Paulin Marius Niamien¹

1. Université Felix Houphouët Boigny, 22 BP 582, Abidjan 22, Côte d'Ivoire.

2. Université Péléforo Gon Coulibaly, BP 1328 Korhogo, Côte d'Ivoire.

Manuscript Info

Manuscript History

Received: 19 May 2021

Final Accepted: 20 June 2021

Published: July 2021

Key words:-

Aluminium, Sulphuric Acid, Corrosion Inhibitor, Tenoxicam, Gravimetric, DFT Calculations, QSPR

Abstract

The inhibiting performances of Tenoxicam against aluminium corrosion in 2M H₂SO₄ have been tested. The results show that inhibition efficiency increases with increase in tenoxicam concentration, but decreases with increasing temperature. The experimental data show that the adsorption process follows the Villamil isotherm. The thermodynamic adsorption and activation functions were determined and analysed. The adsorption of the molecule onto the aluminium surface is an exothermic and spontaneous process. The Adejo-Ekwenchi isotherm indicates a mixed adsorption type, but essentially physisorption at low temperature and chemisorption at high temperature. The global and local molecular descriptors confirmed the existence of a mixed adsorption type. The QSPR studies based on two sets of energetic molecular parameters (E_{HOMO} , E_{LUMO}) and (ΔE , E_{LUMO}) show a good reliability between inhibition efficiency and the mentioned descriptors.

Copy Right, IJAR, 2021., All rights reserved.

Introduction:-

Corrosion [1, 2] is the degradation of a material by chemical or electrochemical reaction in the presence of an aggressive environment. It occurs in variable environments (industrial, urban, rural). It is an important industrial problem: the cost of corrosion covers all the means of combating it, the replacement of corroded parts or structures and the direct and indirect consequences of accidents due to component failure. In summary [3-5], corrosion is a topic that deserves further research in order to understand how the degradation affects our life.

Aluminium [6] is known to be a corrosion resistant metal. However, it can sometimes happen that aluminium corrodes. In contact with an oxygen-containing medium, such as air and water, an oxide surface is created on the aluminium. This protecting layer commonly called alumina, acts as a protective barrier against corrosive atmospheres. This is why aluminium is known for its resistance to corrosion. Even though a natural protective barrier is created on aluminium, there are still conditions that make it possible for corrosion to occur on aluminium parts. It is therefore essential to know the types of corrosion and their propagation mechanisms in order to prevent damage due to corrosion.

Corrosion inhibitors [7-9] are chemical molecules that slow down the corrosion process of metals in a given environment. Usually, they are added in low concentration in the corrosive medium. Thus, corrosion inhibitors constitute a means of combating metal corrosion. This is possible because the treatment is carried out via the

Corresponding Author:- Kalifa Mariko

Address:- Université Felix Houphouët Boigny, 22 BP 582, Abidjan 22, Côte d'Ivoire.

corrosive medium and not on the metal itself. The choice of the inhibitor [10, 11] must comply with the standards and regulations concerning toxicity and the environment. A perusal of the literature [12-15] show that organic molecules with heteroatoms (O, S, N, P...) in their structures are the most effective, economic and practical corrosion inhibitors.

Many techniques can be used to study corrosion inhibition and mechanisms:

Experimentally, gravimetric measurement [16] makes possible to easily determine the speed of corrosion over a relatively long period of time so that the mass loss (link to the inhibition efficiency) induced by the dissolution can be determined with sufficient precision.

Theoretically, understanding the mechanisms of corrosion and corrosion inhibition is therefore a real challenge for research today. In order to get information on the corrosion mechanism, DFT calculations [17-19] are made to illustrate the molecular structures and behaviours of corrosion inhibitors. Various quantum chemical parameters [20-22] can then be obtained to elucidate the adsorption and corrosion inhibition behaviours of the organic molecules. DFT calculations allow gaining insight into the mechanisms by which inhibitors added to aggressive environments retard the metal-environment interaction.

The main objective of this work is to study the performance of Tenoxicam, a nonsteroidal anti-inflammatory drug with analgesic and antipyretic properties as an aluminium corrosion inhibitor in 2M sulphuric acid solution.

Material and Methods:-

Materials

Aluminium specimens

The 95% pure aluminium sample of 10 mm of length and a diameter of 2 mm was obtained from an aluminium bar.

Chemicals

The tested molecule of Tenoxicam (figure 1) was purchased from Sinopharm Chemical Reagent Co Ltd.

Sulfuric acid of purity 95-97 % from Merck was used to prepare the aggressive solutions and acetone of purity 99.5% from Sigma Aldrich for sample surface cleaning. All the chemicals were of analytical grade, so they were used without further purification.

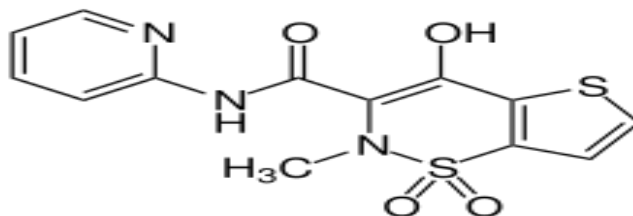


Figure 1:- Structure of Tenoxicam.

Methods:-

Mass loss technique

The mass loss method [23- 25] is one of the most used methods of metal corrosion inhibition assessment due to its simplicity and reliability of measurement. The aluminium samples were cleaned with emery paper, degreased by washing with ethanol, dipped in acetone, removed and dried before use. They were weighed before and after immersion in 50 mL of the acidic solution with or without Tenoxicam. The tests were repeated three times for each solution, at a given temperature and the mean value was recorded. The corrosion rate (W) in $\text{g.cm}^{-2}.\text{h}^{-1}$ was calculated using the below equation:

$$W = \frac{m_1 - m_2}{S \cdot t} \quad (1)$$

Where m_1 and m_2 are respectively the mass of the sample before and after immersion. S is the sample total surface and t is the immersion time.

The inhibition efficiency is given by the following equation:

$$\text{IE}(\%) = \frac{W_0 - W}{W_0} \quad (2)$$

Density Functional Theory

The theoretical calculations were performed, using the Density Functional Theory at B3LYP/ 6-31G (d) level, which led to total energy of the studied molecule (Tenoxicam) with a good precision with an acceptable CPU time. The molecular parameters as HOMO and LUMO energies and dipole moment (μ) were obtained. Many other parameters have been deduced from the first ones. So, we determined the energy gap (ΔE), the electron affinity (A), the ionization potential (I), the Chemical hardness (η), the chemical softness (S), the electronegativity (χ), the chemical potential (μ_p) and the electrophilicity index (ω). The expressions of these parameters are given below:

$$\Delta E = E_{\text{LUMO}} - E_{\text{HOMO}} \quad (3)$$

$$I = -E_{\text{HOMO}} \quad (4)$$

$$A = -E_{\text{LUMO}} \quad (5)$$

$$\eta = \frac{I-A}{2} \quad (6)$$

$$S = \frac{1}{\eta} \quad (7)$$

$$\chi = -\mu_p = \frac{I+A}{2} \quad (8)$$

$$\omega = \frac{\mu_p}{2\eta} \quad (9)$$

To get insight into the reactivity of each atom in the molecule, we used the condensed Fukui functions [26, 27], which is defined as the change of the charge for a given atom in relation to change of the total number of electrons in the molecule. This function is defined as:

$$f_k = -\left(\frac{\partial q_k}{\partial N}\right)_{v(r)} \quad (10)$$

Where q_k is the charge of the atom, referring to Mulliken population. The electrophilic and nucleophilic functions are:

$$f_k^+ = q_k(N+1) - q_k(N) \quad (11)$$

$$f_k^- = q_k(N) - q_k(N-1) \quad (12)$$

Where N+1, N and N-1 are respectively the number of electrons calculated for the same symmetry in the case of positive and negative charge species. Even if the Fukui function has the capability to reveal nucleophilic and electrophilic region on a molecule only the dual descriptor $\Delta f_k(r)$ [28] is able to unambiguously expose truly nucleophilic and electrophilic regions:

$$\Delta f_k(r) = f_k^+(r) - f_k^-(r) \quad (13)$$

This descriptor can be considered as the most reliable descriptor to measure local reactivity.

QSPR method

Quantitative Structure Property Relationship (QSPR) is a mathematical link between a physical or chemical property and the molecular structure through molecular parameters. The chemical structure is represented by some sets of descriptors that can mathematically be connected to experimental properties. In this work we tried to correlate some sets of composite index with experimental corrosion inhibition efficiency of tenoxicam. Multiple linear regression models [29] was used for the study of the interaction of the studied molecule with the aluminium surface in the hydrochloric acid solution. We used the relation based on the direct linear relationship which is given below:

$$IE(\%) = Ax_j C_i + B \quad (10)$$

Where x_j is a molecular parameter while A and B are real constants in the mathematical model and C_i is the concentration of the studied molecule.

Results And Discussion:-

Effects of concentration and temperature

Figures 1 and 2 give us the influence of the concentration of the studied molecule and the temperature of the medium on the inhibition efficiency.

In these figures, one can see that for $C = 10^{-5} \text{ M}$ and $C = 10^{-2} \text{ M}$:

- At T = 298K, the values of inhibition efficiency IE (%) are respectively 66.7 and 94.95.
- At T = 338K, the values of inhibition efficiency IE (%) are respectively 21.74 and 55.07.

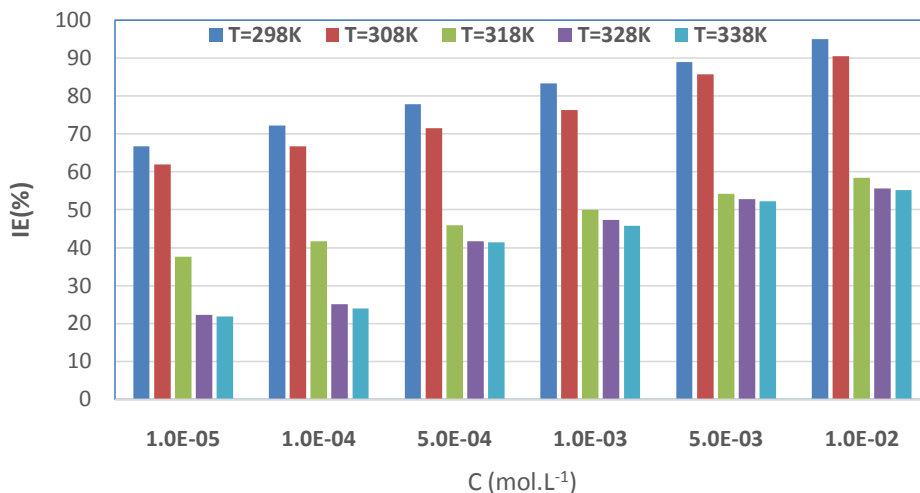


Figure 1:- Inhibition efficiency versus concentration for different temperatures.

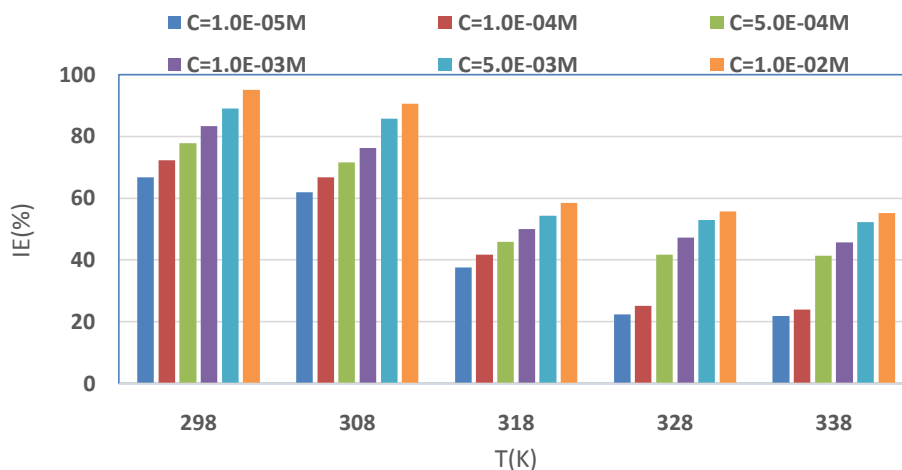


Figure 2:- Inhibition efficiency versus temperature for different concentrations.

Analysing figures 1 and 2, one can see that the inhibition efficiency of the studied molecule depends on the value of both its concentration and the temperature of the environment. The inhibition efficiency increases with increasing concentration, what can be explained by the increase in surface coverage. The decrease in the inhibition efficiency with increasing temperature could be associated with an increase in desorption of the organic molecule. The presence of the molecule decreases the corrosion phenomenon but doesn't stop it. So, the activation parameters for the corrosion process were calculated, using the following equation: $W = k \exp\left(-\frac{E_a}{RT}\right)$ (11)

$$W = \frac{RT}{\aleph h} \exp\left(\frac{\Delta S_a}{R}\right) \exp\left(-\frac{\Delta H_a}{RT}\right) \quad (12)$$

These equations can be taken in the two following forms:

$$\log W = \log k - \frac{E_a}{2.3RT} \quad (13)$$

$$\log\left(\frac{W}{T}\right) = \log\left(\frac{R}{\aleph h}\right) + \frac{\Delta S_a}{2.3R} - \frac{\Delta H_a}{2.3RT} \quad (14)$$

Where R is the universal gas constant, T is the absolute temperature, \aleph is the Avogadro's number and h is the Planck's constant. The plots of $\log W = f(1/T)$ and $\log(W/T) = g(1/T)$ (Figures 3 and 4) led to the activation parameters (E_a , ΔH_a , ΔS_a).

E_a and ΔH_a were obtained respectively from the slopes of the straight lines associated to (13) and (14), while ΔS_a derived from the intercept of the straight line obtained with equation (13).

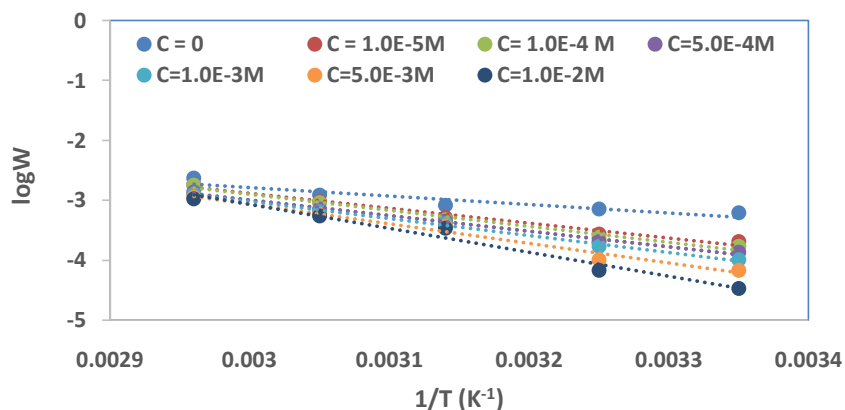


Figure 3:- $\log W$ versus $1/T$ for different concentrations.

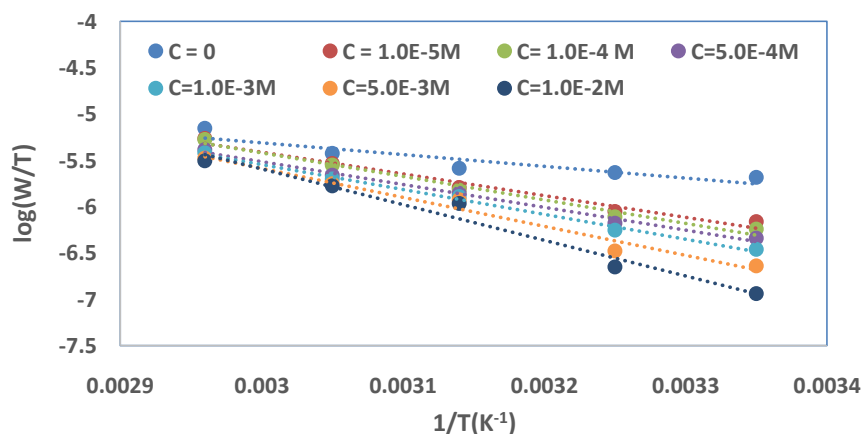


Figure 4:- $\log(W/T)$ versus $1/T$ for different concentrations.

All the activation parameters are listed in Table 1.

Table 1:- Activation parameters of aluminium corrosion in 2M H_2SO_4 for different concentrations.

C (M)	E_a (kJmol^{-1})	ΔH_a (kJmol^{-1})	ΔS_a ($\text{Jmol}^{-1}\text{K}^{-1}$)
0	26.9	24.2	-226.0
1.0E-5	47.6	44.9	-165.8
5.0E-4	51.1	48.4	-155.6
1.0E-4	49.8	47.1	-161.3
5.0E-3	54.1	51.5	-148.8
1.0E-3	62.4	59.7	-124.8
1.0E-2	76.2	73.6	-83.5

The value of E_a increase with increasing concentration in Tenoxicam; inspection of the values reveals that E_a for the solutions containing Tenoxicam are higher than that of the blank, what indicates [30] that physical adsorption is the mean adsorption type.

The obtained values of ΔH_a are in good agreement with the calculated values from the equation below:

$$\Delta H_a = E_a - RT \quad (15)$$

The positive sign of the variation of activation enthalpy (ΔH_a) [31] shows that the dissolution of aluminium is an endothermic process, whereas the negative sign of the variation of activation entropy (ΔS_a) indicates that the activation complex represents an association rather than a dissociation. The increase in (ΔS_a) could be explained by the substitution of water molecules by the molecule of Tenoxicam.

Adsorption isotherms

The capability of an organic molecule to reduce the corrosion of a metal depends on its ability to adsorb on the metallic surface. So, it is very important to know the adsorption mechanism given through the adsorption models. We have tested many models but the best model is that of Langmuir.

Langmuir adsorption isotherm

The mathematical relation which expressed this adsorption isotherm is:

$$\frac{C}{\theta} = \frac{1}{K_{ads}} + C \quad (16)$$

Where C is the inhibitor's concentration, θ is the degree of surface coverage and K_{ads} is the equilibrium constant. Table 1 gives the equations and the correlation coefficient of the straight lines. Figure 5 gives the plots of $\frac{C}{\theta}$ versus C.

Table 1:- Equation and correlation coefficient of the Langmuir model.

T(K)	Equation	R ²
298	$C/\theta = 1.0551C + 0.0001$	0.999
308	$C/\theta = 1.1033C + 0.0001$	0.999
318	$C/\theta = 1.7168C + 0.0002$	0.999
328	$C/\theta = 1.7888C + 0.0003$	0.999
338	$C/\theta = 1.7741C + 0.0005$	0.996

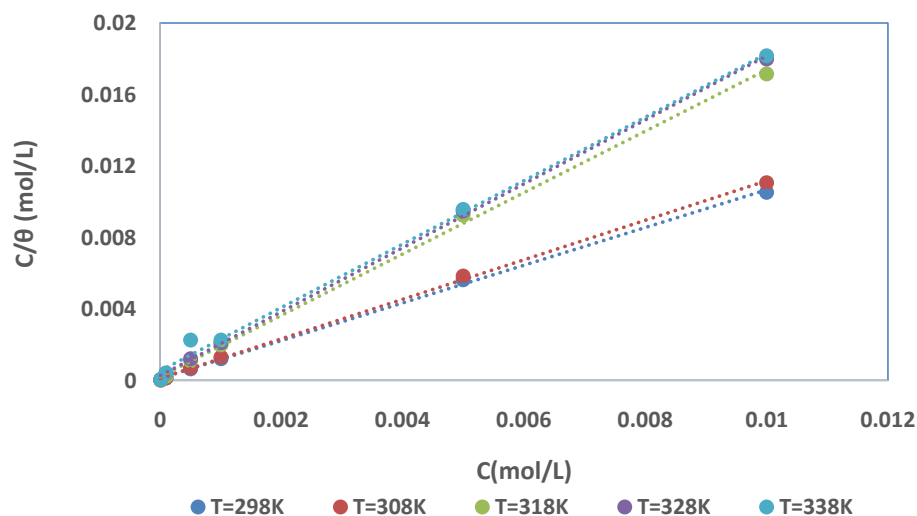


Figure 5:- Langmuir adsorption isotherm for Tenoxicam on aluminium surface.

The plots are straight lines with correlation coefficient near unity. However, the slopes are different from unity, which does not allow the Langmuir isotherm to be applied rigorously. Therefore, the modified Langmuir isotherm known as Villamil isotherm [32] is used. The equation of this isotherm is:

$$\frac{C}{\theta} = \frac{n}{K_{ads}} + C \quad (17)$$

Thermodynamic adsorption functions

The change in free adsorption enthalpy is obtained from the equation below:

$$\Delta G_{ads}^0 = -RT \ln(55.5 K_{ads}) \quad (18)$$

Where R is the gas constant, T is the absolute temperature and 55.5 is the concentration of water (in mol.L⁻¹) in the solution. The changes in enthalpy (ΔH_{ads}^0) and entropy (ΔS_{ads}^0) are related to the change in free adsorption enthalpy by the basic equation below:

$$\Delta G_{\text{ads}}^0 = \Delta H_{\text{ads}}^0 - T\Delta S_{\text{ads}}^0 \quad (19)$$

Figure 6 gives the plot of ΔG_{ads}^0 versus T. The plot is a straight line with a slope ($-\Delta S_{\text{ads}}^0$) and an intercept (ΔH_{ads}^0). The obtained values are listed in Table 2.

ΔG_{ads}^0 and ΔH_{ads}^0 are negative, showing a spontaneous and exothermic adsorption process. The change in adsorption entropy has also a positive sign, what indicates an increase in disorder due to desorption of water molecules.

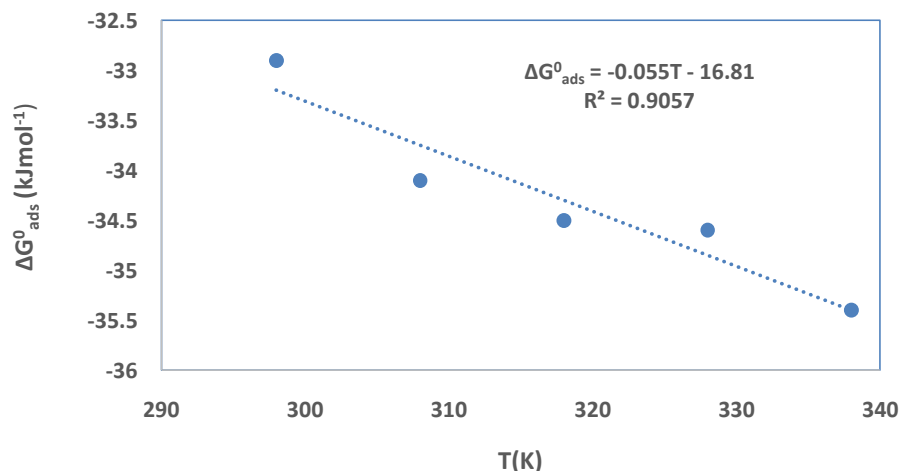


Figure 6:- Change in free adsorption enthalpy versus temperature.

Table 2:- Values of the adsorption thermodynamic functions.

T(K)	K_{ads} (M ⁻¹)	$-\Delta G_{\text{ads}}^0$ (kJmol ⁻¹)	ΔH_{ads}^0 (kJmol ⁻¹)	ΔS_{ads}^0 (Jmol ⁻¹ K ⁻¹)
298	10551.0	32.9	-16.8	55
308	11033.0	34.1		
318	8584.0	34.5		
328	5962.7	34.6		
338	5300.2	35.4		

Adsorption type

Analysing the values of the change in adsorption free enthalpy (ΔG_{ads}^0) nearer -40kJmol^{-1} , one can see [33] that the adsorption is more physisorption than chemisorption. In order to access other information about the adsorption type, we used the Adejo-Ekwenchi adsorption isotherm which equation is:

$$\log\left(\frac{1}{1-\theta}\right) = \log K_{\text{AE}} + \log C \quad (20)$$

Where K_{AE} and b are the parameters of the isotherm and C, the adsorbate concentration.

Figure 7 gives the plots of $\log(1/1 - \theta)$ versus $\log C$ and the values of all the related parameters are listed in Table 3.

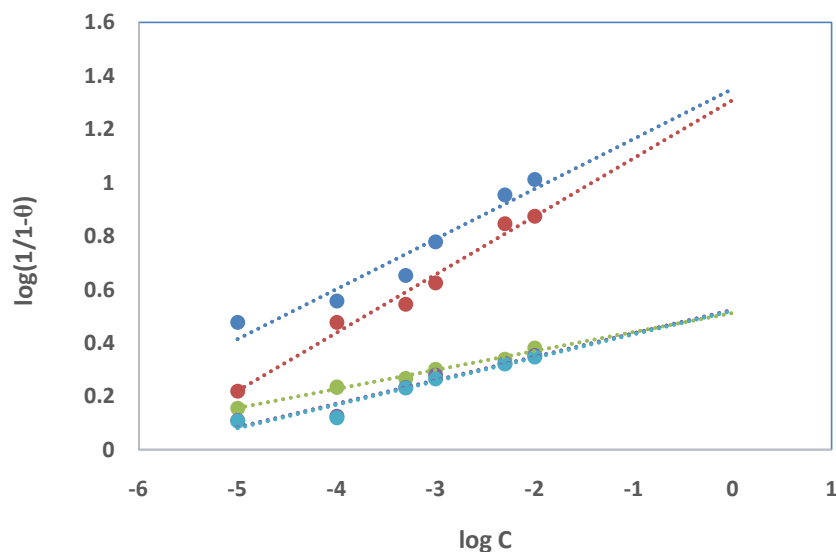


Figure 7:- Adejo-Ekwenchi isotherm for Tenoxicam on aluminium surface.

Table 3:- Adejo-Ekwenchi adsorption isotherm parameters.

T(K)	Equation	K_{AE}	b	R^2
298	$\log\left(\frac{1}{1-\theta}\right) = 0.2398\log C + 1.4908$	30.96	0.2398	0.966
308	$\log\left(\frac{1}{1-\theta}\right) = 0.2179\log C + 1.3089$	20.36	0.2179	0.921
318	$\log\left(\frac{1}{1-\theta}\right) = 0.0714\log C + 0.5125$	3.25	0.0714	0.972
328	$\log\left(\frac{1}{1-\theta}\right) = 0.0882\log C + 0.5246$	3.34	0.0882	0.925
338	$\log\left(\frac{1}{1-\theta}\right) = 0.0879\log C + 0.5188$	3.30	0.0879	0.936

In the temperature range from 298K to 318K, we observed a decrease in b values, what [34] indicates that adsorption type is physisorption. From T = 318K to T = 338K, one can see that b is fairly constant, showing [35] that chemisorption is the adsorption type. Globally, the main adsorption type is physisorption.

Theoretical studies

Global molecular parameters

Global parameters of Tenoxicam have been calculated, using Gaussian 09, with B3LYP/6-31G (d) method. All these parameters are listed in Table 4.

Table 4:- Global molecular parameters of Tenoxicam by B3LYP/6-31 G (d).

Parameter	Value	Parameter	Value
E_{HOMO} (eV)	-6.276	A(eV)	2.410
E_{LUMO} (eV)	-2.410	η (eV)	1.933
ΔE (eV)	3.866	S (eV) ⁻¹	0.517
μ (D)	3.458	χ (eV) = $-\mu_p$	4.343
I(eV)	6.276	ω (eV)	4.878

The parameter E_{HOMO} (energy of the highest occupied molecular orbital) corresponds to the area in the molecule where electrons can be given to electrophile systems; thus, the higher, the value, the higher the tendency of the molecule to donate electrons to an appropriate acceptor. In our case the Tenoxicam, with E_{HOMO} (-6.276 eV) can be considered [36] as a good electrons donor. On the other hand, E_{LUMO} , the energy of the lowest unoccupied molecular orbital is the energy of the region in the molecule that has the greatest propensity to accept electrons. The value of this parameter in our molecule is (-2.410 eV), indicating [36] a good acceptor capacity.

The energy gap HOMO-LUMO is an important parameter that need to be considered. Lower values of this energy [37] lead to higher reactivity tendency, indicating good inhibition efficiency. For the studied molecule, the value of the energy gap ($\Delta E = 3.866$ eV) can be considered [38, 39] as low when comparing to values in the literature.

The dipole moment (μ) result from non-uniformity in the charges distribution in the molecule. Though this parameter is important, there is [40] irregularities in the correlation between it and the inhibition efficiency.

Hardness (η) and softness (σ) are two other reactivity parameters that give information on the ability or not of the molecule to give or receive electrons. A high value of hardness (low value of softness) [41, 42] leads to a low value of inhibition efficiency while a low value of hardness (high value of softness) indicates a good inhibition performance. In our work, the values of hardness ($\eta = 1.933$ eV) and softness ($\sigma = 0.517$ eV⁻¹) can respectively be considered as low and high, what explain the high value of inhibition efficiency (IE (%) = 94.5 for C = 10⁻² M and T = 298K).

The electronegativity (χ) and the electrophilicity index (ω) [43] are related to the capacity of the molecule to accept electrons. So, high values of these parameters lead to good inhibition efficiency. The obtained values from the quantum chemical calculations ($\chi = 4.343$ eV) and ($\omega = 4.878$ eV) that are high values justify the good inhibition character of Tenoxicam.

The fraction of electrons transferred (ΔN) was calculated, using Pearson's equation [44]:

$$\Delta N = \frac{(\phi_{Al} - \chi_{inh})}{2(\eta_{Al} + \eta_{inh})} \quad (21)$$

Where ϕ_{Al} is the work function of the aluminium surface, χ_{inh} is the absolute electronegativity of the inhibitor, η_{Al} and η_{inh} are respectively the absolute hardness of the aluminium and the inhibitor. In this work we used $\phi_{Al} = 4.28$ eV and $\eta_{Al} = 0$ [45]. The negative value of ΔN (-0.016) indicates that the molecule have rather tendency to receive electrons from the metal.

Local reactivity parameters

The local reactivity was studied, using Fukui's functions, which are related to reactivity of regions in the molecule: one can find nucleophilic or electrophilic character of the molecule in a specified region. The region of nucleophilic or electrophilic behaviour is affected by a large Fukui function value.

It has been proved [46, 47] that the dual descriptor described well the reactivity, combining Fukui functions. So, the condensed dual descriptor over atomic sites, indicates a process driven by a nucleophilic attack on atom k when $\Delta f_k > 0$ (atom k reacts as an electrophilic species) and a process driven by an electrophilic attack when $\Delta f_k < 0$ (atom k reacts as a nucleophilic species). Figures 8 and 9 give respectively the structure and the HOMO and LUMO orbitals of Tenoxicam while Table 5 presents Fukui and dual functions.

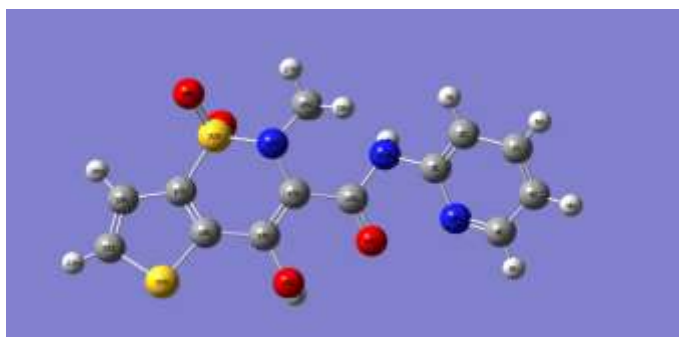


Figure 8:- Structure of Tenoxicam by B3LYP/6-31 G(d).

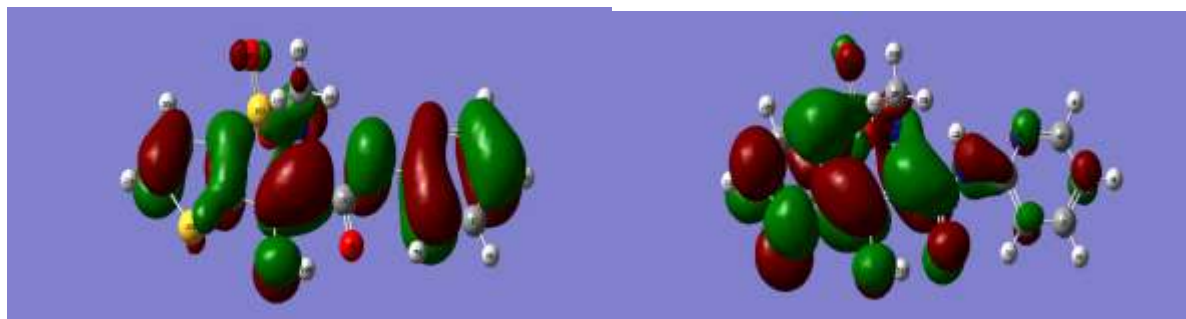


Figure 9:- HOMO (left) and LUMO (right) orbitals of Tenoxicam by B3LYP/6-31G (d).

Table 5:- Fukui and dual functions of atoms in Tenoxicam, obtained using Mulliken charges.

Atom	$q_k(N+1)$	$q_k(N)$	$q_k(N-1)$	f_k^+	f_k^-	Δf_k
1 C	-0.120048	-0.114189	-0.096354	-0.005859	-0.017835	0.011976
2 C	-0.159924	-0.150373	-0.170976	-0.009551	0.020603	-0.030154
3 C	0.493286	0.494369	0.489866	-0.001083	0.004503	-0.005586
4 C	0.039671	0.044899	0.047278	-0.005228	-0.002379	-0.002849
5 C	-0.158142	-0.141804	-0.132359	-0.016338	-0.009445	-0.006893
6 H	0.112111	0.148561	0.182828	-0.03645	-0.034267	-0.002183
7 H	0.180465	0.189827	0.163805	-0.009362	0.026022	-0.035384
8 H	0.10956	0.147439	0.1809	-0.037879	-0.033461	-0.004418
9 H	0.097776	0.140162	0.179715	-0.042386	-0.039553	-0.002833
10 N	-0.511383	-0.499404	-0.439396	-0.011979	-0.060008	0.048029
11 N	-0.717536	-0.712005	-0.692262	-0.005531	-0.019743	0.014212
12 H	0.35686	0.373895	0.365653	-0.017035	0.008242	-0.025277
13 C	0.602161	0.664672	0.667164	-0.062511	-0.002492	-0.060019
14 O	-0.662326	-0.607622	-0.52922	-0.054704	-0.078402	0.023698
15 C	0.056621	0.105375	0.235375	-0.048754	-0.13	0.081246
16 C	0.344145	0.367619	0.381381	-0.023474	-0.013762	-0.009712
17 C	-0.191153	-0.16065	-0.154003	-0.030503	-0.006647	-0.023856
18 C	-0.20326	-0.183455	-0.182423	-0.019805	-0.001032	-0.018773
19 C	-0.104762	-0.106248	-0.090021	0.001486	-0.016227	0.017713
20 H	0.134134	0.186388	0.229176	-0.052254	-0.042788	-0.009466
21 C	-0.372581	-0.342266	-0.317985	-0.030315	-0.024281	-0.006034
22 H	0.128114	0.19438	0.247208	-0.066266	-0.052828	-0.013438
23 O	-0.683128	-0.635565	-0.567047	-0.047563	-0.068518	0.020955
24 H	0.434461	0.458121	0.489234	-0.02366	-0.031113	0.007453
25 N	-0.647138	-0.659971	-0.644321	0.012833	-0.01565	0.028483
26 C	-0.303098	-0.322402	-0.365892	0.019304	0.04349	-0.024186
27 H	0.148625	0.163467	0.250101	-0.014842	-0.086634	0.071792
28 H	0.149888	0.176217	0.230294	-0.026329	-0.054077	0.027748
29 H	0.17293	0.208416	0.215535	-0.035486	-0.007119	-0.028367
30 O	-0.57596	-0.526299	-0.457121	-0.049661	-0.069178	0.019517
31 O	-0.522725	-0.485936	-0.427555	-0.036789	-0.058381	0.021592
32 S	1.187416	1.242053	1.252085	-0.054637	-0.010032	-0.044605
33 S	0.18494	0.342329	0.45934	-0.157389	-0.117011	-0.040378

Analysing the dual functions, one can see that in Tenoxicam, the probable electrophilic attack centre is C (13) with $\Delta f_k < 0$, while the probable nucleophilic attack centre is C (15) with $\Delta f_k > 0$.

QSPR studies

QSPR is the focus of many studies that aim to model and predict molecular properties. The performance of QSPR model depends on the parameters used to describe the molecular structure. We tried many sets of two parameters. Only two sets based on the energetic molecular parameters lead to good results.

(E_{HOMO} , E_{LUMO})

The mathematical relation is:

$$IE(\%) = AC_i E_{\text{HOMO}} + BC_i E_{\text{LUMO}} + D \quad (22)$$

(ΔE , E_{HOMO})

The mathematical relation is:

$$IE(\%) = AC_i \Delta E + BC_i E_{\text{HOMO}} + D \quad (23)$$

The real constant are determined using Excel software. Table 6 gives the real constants for the different sets

Table 6:- real constants obtained for two different sets.

C_i (μM)	$(E_{\text{HOMO}}, E_{\text{LUMO}})$			$(\Delta E, E_{\text{HOMO}})$		
	A	B	D	A	B	D
10	3.0680	-15.4240	-113.5	-15.4240	-12.356	-113.5
100	0.1610	-0.9920	-66.076	-0.9920	-0.830	-66.076
500	0.0170	-0.1420	-40.059	-0.1420	-0.125	-40.059
1000	0.0080	-0.0710	-35.773	-0.0700	-0.063	-40.523
5000	-0.0013	-0.0031	11.446	-0.0031	-0.0044	11.446
10000	-0.0014	0.0012	37.338	0.0012	-0.0002	37.338

Figures 10 and 11 give the representations of experimental inhibition efficiency versus theoretical ones.

The representations are straight lines with slopes near unity. In order to determine the best set, we use correlation coefficient (R^2) and a statistical analysis based on sum of square errors (SSE), root mean square error (RMSE) and mean percent deviation (MPD).

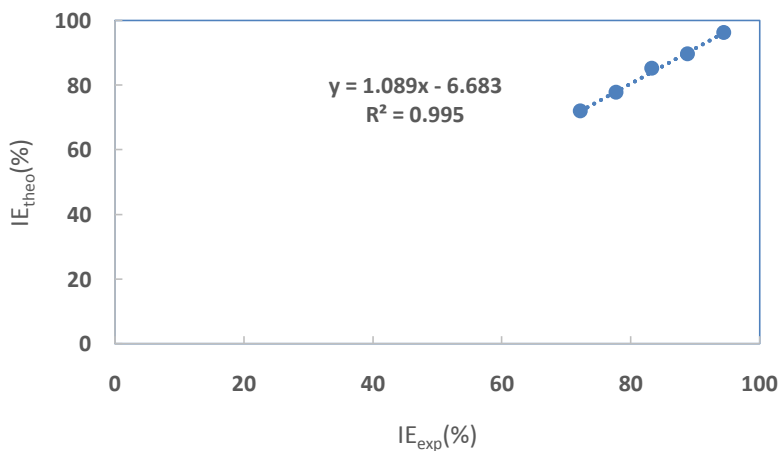


Figure 10:- I_{theo} (%) versus I_{exp} for (E_{HOMO} , E_{LUMO}).

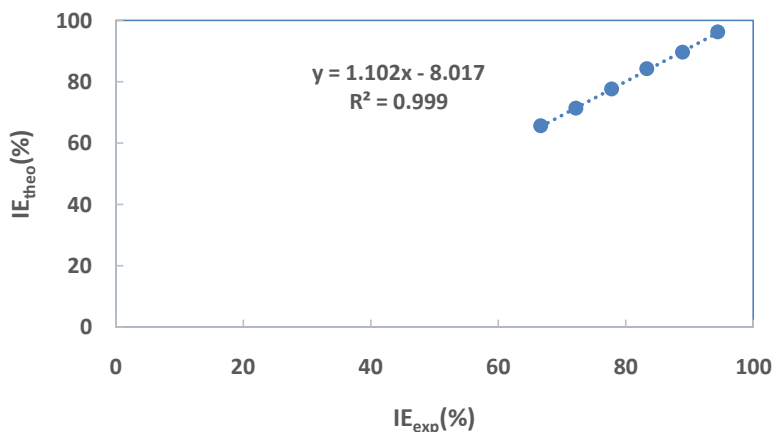


Figure 11:- I_{theo} (%) versus I_{exp} for $(\Delta E, E_{\text{LUMO}})$.

The relations of the statistical parameters are given below:

$$\text{SSE} = \sum_{i=1}^N [\text{IE}_{\text{theo}}^i (\%) - \text{IE}_{\text{exp}}^i (\%)]^2 \quad (24)$$

$$\text{RMSE} = \sqrt{\frac{\sum_{i=1}^N |\text{IE}_{\text{exp}}^i - \text{IE}_{\text{theo}}^i|}{N}} \quad (25)$$

$$\text{MPD} = \frac{1}{N} \sum_{i=1}^N \left| \frac{\text{IE}_{\text{exp}}^i - \text{IE}_{\text{theo}}^i}{\text{IE}_{\text{exp}}^i} \right| \quad (26)$$

Table 7:- Statistical parameters of the two sets.

Set	SSE	RMSE	MPD	R^2
$(E_{\text{HOMO}}, E_{\text{LUMO}})$	8.39	0.99	0.012	0.995
$(\Delta E, E_{\text{LUMO}})$	6.51	0.92	0.011	0.999

Analysing the values of correlation coefficients and that of the statistical parameters (SSE, RMSE and MPD), one can see that even if $(\Delta E, E_{\text{LUMO}})$ is the best set, QSPR models based on the two sets have good reliability with experimental data.

Conclusion:-

The inhibition efficiency of Tenoxicam towards corrosion of aluminium in 2M H_2SO_4 has been evaluated, using mass loss, Density Functional Theory (DFT) and Quantitative Structure Property Relationship (QSPR). The results obtained from mass loss technique show that inhibition efficiency increases with increasing concentration, but decreases when the temperature increases. The change in free adsorption enthalpy is negative, implying the spontaneity of the adsorption and the stability of the adsorbed layer on the aluminium surface. ΔG_{ads}^0 values were laying between -40 kJ mol^{-1} and -20 kJ mol^{-1} , indicating a mixed adsorption process. The values of change in activation enthalpy and the evolution of activation energy with the inhibitor concentration show that physisorption is the main adsorption type. The global and local descriptors and the QSPR studies are in good agreement with the inhibition efficiency.

References:-

- [1] Fontana, M. G. (1987). Corrosion engineering, Third Edition, McGraw-Hill International Edition, New York
- [2] Cimitha, A., Umesha P. K., Ieyer N. R. (2014). An Overview of Corrosion and Experimental Studies on Corroded Mild Steel compression Members. KSCE Journal of Civil Engineering, 18(6): 1735-1744.

- [3] Natesan, M., Venkatachari, G., and Palaniswamy, N. (2006). "Kinetics of atmospheric corrosion of mild steel, zinc, galvanized iron and aluminium at 10 exposure stations in India." *Corrosion Science*.48 (11): 3584-3608.
- [4] Natesan, M., Venkatachari, G., Palaniswamy, N., and Rajeswari, A. (2008). "A novel approach to updating the corrosiveness maps of India." *Corrosion the Journal of Science and Engineering*. 64(2): 92-100.
- [5] Landolfò, R., Cascini, L., and Portioli, F. (2010). "Modelling of metal structure corrosion damage: A state of the art report." *Sustainability*.2(2): 2163-2175.
- [6] Klodian X., Matjaz, F., Masa K. N., Uros M. Zeljko K., Bujar S. (2017). Green Corrosion inhibitors for aluminium and its alloys: a review. *RSC. Adv*.7: 27299-27330.
- [7] Obot, I. B., Obi-Egbedi, N. O., Umoren, S. A. (2009). Antifungal drugs as corrosion inhibitors for aluminium in 0.1 M HCl. *Corrosion Science*. 51(8):1868-1875.
- [8] El-Etre, A., Y., Shahera, M., Shohayeb, M. A., Elkomy, S., Abdelhamed, S. (2016). Inhibition of acid aluminium corrosion in presence of aqueous extract of Domiana. *Journal of Basic and Environmental Sciences*. 3 (1):25-36.
- [9] Adejoro, I. A., Akintayo, D. C., Ibeji, C. U. (2016). The efficiency of chloroquine as corrosion inhibitor for aluminium in 1M HCl solution: Experimental and DFT study. *Jordan Journal of Chemistry*.11 (1):38-49.
- [10] Yurt, A., Balaban A., Kandemir, S. U., Bereket, G., Erk B. (2004). Investigation on some Schiff bases as HCl corrosion inhibitors for carbon steel. *Materials Chemistry and Physics*. 85 (2-3): 420-426.
- [11] Ladha, D. G., Naik, U. J., Shah, N. K. (2013). Investigation of cumin (*Cuminum cyminum*) extract as an eco-friendly green corrosion inhibitor for pure Aluminium in acid medium. *Journal of Materials and Environmental Science*.4(5):701-708.
- [12] Obot, I.B., Obi-Egbedi, N.O. (2010). Theoretical study of benzimidazole and its derivatives and their potential activity as corrosion inhibitors, *Corros. Sci*. 52 (2): 657-660.
- [13] Obi-Egbedi, N.O., Obot, I.B., El-Khaiary, M.I. (2011). Quantum chemical investigation and statistical analysis of the relationship between corrosion inhibition efficiency and molecular structure of xanthene and its derivatives on mild steel in sulphuric acid, *J. Mol. Struct*. 1002 (1-3): 86-96.
- [14] Ebenso, E.E., Kabanda, M.M., Arslan T., Saracoglu M., Kandemirli, F., Murulana, L.C. Singh, A.K., Shukla, S.K., Hammouti B., Khaled, K.F., Quraishi M.A., Obot, I.B. Eddy, N.O. (2012). Quantum chemical investigations on quinoline derivatives as effective corrosion inhibitors for mild steel in acidic medium. *Int. J. Electrochem. Sci*. 7 (6): 5643-5676.
- [15] M.M. Kabanda, Murulana, L.C., M.Ozcan, Karadag F., Dehri, I. B. Obot, E.E. Ebenso. (2012). Quantum Chemical Studies on the corrosion inhibition of mild steel by some triazoles and benzimidazole derivatives in acidic medium, *Int. J. Electrochem. Sci*. 7 (6): 5035-5056.
- [16] Prieto, C., Gallardo-González, J., Ruiz-Cabañas, F. J., Barreneche, C., Martínez, M., Segarra, M., & Fernández, A. I. (2016). Study of corrosion by Dynamic Gravimetric Analysis (DGA) methodology. Influence of chloride content in solar salt. *Solar Energy Materials and Solar Cells*. 157: 526-532.
- [17] Nagy, A. (1998). Density functional theory and application to atoms and molecules. *Physics Review*. 298: 1-79.
- [18] Becke, A. D. (1986). Density functional calculation of molecular bond energies. *The journal of Chemical Physics*. 84 (8): 4524-4529.
- [19] Hsissou, R., About, S., Seghiri, R., Rehioui, M., Berisha, A., Erramli, H., Assouag, M., Elharfi, A. (2020). Evaluation of corrosion inhibition performance of phosphorus polymer for carbon steel in [1 M] HCl: Computational studies (DFT, MC and MD simulations). *J. Mater. Res. Technol*. 9(3): 2691-2703.
- [20] Ahmed, M. H. O., Al-Amiery, A. A., Al-Majedy, Y. K., Kadhum, A. A. H., Mohamad, A. B., & Gaaz, T. S. (2018). Synthesis and characterization of a novel organic corrosion inhibitor for mild steel in 1 M hydrochloric acid. *Results in Physics*, 8:728-733.
- [21] Al-Fakih, A. M., Abdallah, H. H., & Aziz, M. (2019). Experimental and theoretical studies of the inhibition performance of two furan derivatives on mild steel corrosion in acidic medium. *Materials and Corrosion*, 70(1): 135-148.
- [22] Gece, G. (2015). Corrosion inhibition behaviour of two quinoline chalcones: insights from density functional theory. *Corrosion Reviews*. 33(3-4): 195- 202.
- [23] Khadom, A. A., Yaro, A. S. & Kadum, A. A. H. (2010). Corrosion inhibition by naphthylamine and phenylenediamine for the corrosion of copper-nickel alloy in hydrochloric acid. *Journal of the Taiwan Institute of Chemical Engineers*. 41(1):122-125.
- [24] Musa, A. Y., Khadom, A. A., Kadhum, A. A. H., Mohamad, A. B. & Takriff, M. S. (2010). Kinetic behavior of mild steel corrosion inhibition by 4-amino-5-phenyl-4H-1, 2, 4-triazole-3-thiol. *Journal of the Taiwan Institute of Chemical Engineers*. 41(1): 126-128.
- [25] Rahim, A. & Kassim, J. (2008). Recent Development of Vegetal Tannins in Corrosion Protection of Iron and Steel. *Recent Patents on Materials Science*. 1(3):223-231.

- [26] Shu-Bin, L. (2009). Conceptual Density Functional Theory and Some Recent Developments. *Acta Phys. -Chim. Sin.*, 25:590-600.
- [27] Glossman-Mitnik, D. (2013). Computational Study of the Chemical Reactivity Properties of the Rhodamine B Molecule, *Procedia Comput. Sci.* 18: 816-825.
- [28] Morell C., Grand A., Toro-Labbé A. (2005). New dual descriptor for chemical reactivity, *J. Phys. Chem. A.* 109: 205-212.
- [29] Eddy N.O., Ita B.I. (2011). QSAR DFT and quantum chemical studies on the inhibition potentials of some carbozones for the corrosion of mild steel in HCl. *J. Mol. Model.* 17: 359-376.
- [30] Ramesh S. V., Adhikari A. V. (2009). N³-[4-(diethylaminobenzylidene)-3-([8-(trifluoromethyl)quinolin-4yl]thio) propano hydrazide) as an effective inhibitor of mild steel corrosion in acid media. *Mater. Chem. Phys.* 115: 618-627.
- [31] Abdallah M., HELAL E.A., Fouda A. S. (2006). Amino pyrimidine derivatives as inhibitors for corrosion of 1018 Carbon Steel in nitric acid solution. *Corrosion Science.* 48(7): 1639-1654.
- [32] Villamil R. F. V, Corio P, Rubin J. C., Agostinho S.M.I. (1999). Effect of sodium dodecylsulfate on Copper Corrosion in sulfuric acid media in the absence and presence of benzotriazole. *Electroanalytical Chemistry.* 472: 112-119.
- [33] Chauhan L.R., Gunasekaran G. (2007). Corrosion inhibition of mild steel by plant extract in dilute HCl medium. *Corrosion Sci.* 49 (3): 1143-1161.
- [34] Adejo S. O., Ekwenchi M. M. (2014). Proposing a new empirical adsorption isotherm known as Adejo-Ekwenchi isotherm. *J. Appl. Chem.* 6: 66-71
- [35] Adejo S. O., Ekwenchi M. M. Olatunde P. O., Agbajeola F. (2014). Adsorption Characteristics of ethanol root extract of *Portucula oleracea* as eco-friendly inhibitor of corrosion of mild steel in H₂SO₄. *J. Appl. Chem.* 7(4): 55-60.
- [36] Popova A., Christov M., Deligeorgiev T. (2003). Influence of the Molecular Structure on the corrosion properties of Benzimidazole Derivatives on Mild Steel Corrosion in 1M Hydrochloric Acid. *Corrosion.* 59(9): 756-764.
- [37] Issa R. M., Awad M. K. (2008). "Quantum Chemical studies on the inhibition of corrosion of copper surface by substituted Uracils". *Appl. Surf. Sci.* 255 (5): 2433-2441.
- [38] Obot I. B., Obi-Egbedi N. O. (2008). Inhibitory effect and adsorption characteristics of 2, 3-diaminonaphthalene at aluminium/hydrochloric acid interface: Experimental and Theoretical study, *Surface Review and Letters*, 15(6): 903-910.
- [39] Döner A., Solmaz R., Özcan M., Karas G. (2011). Experimental and Theoretical studies of Thiazoles as corrosion inhibitors for mild steel in sulphuric acid solution, *Corrosion Science*, 53 (9): 2902-2913.
- [40] Gece. G. (2008). The use of quantum chemical methods in corrosion inhibitors studies, *Corros. Sci.*, 50 (11): 2981-2992.
- [41] Obi-Egbedi N. O., Obot I. B., El-Khaiary M. I., Umoren S. A., Ebenso E. E. (2011). Computational Simulation and Statistical Analysis on the Relationship between Corrosion Inhibition Efficiency and Molecular Structure of Some Phenanthroline Derivatives on Mild Steel Surface, *Int. J. Electrochem. Sci.* 6 (11): 5649-5675.
- [42] Gece G., Bilgiç S. (2009). Quantum chemical study of some cyclic nitrogen compounds as corrosion inhibited of steel in NaCl media, *Corros. Sci.*, 51(8): 1876-1878.
- [43] Parr R. G., Szentpaly L., Liu S. (1999). Electrophilicity index, *J. Am. Chem. Soc.*, 121 (9): 1922-1924.
- [44] Pearson R. G. (1990). *Coordination Chemistry Reviews* 100: 403-425.
- [45] Kokalj A., Kovacevic N. (2011). On the consistent use of electrophilicity index and HSAB-based electron transfer and its associated change of energy parameters, *Chemical Physics Letters*, 507 (1-3): 181-184.
- [46] Chamorro, E., Pérez, P., Domingo, L. R. (2013). On the nature of Parr functions to predict the most reactive sites along organic polar reactions. *Chem. Phys. Lett.* 582 : 141-143.
- [47] Domingo, L. R., Pérez, P., Sáez, J. (2013). Understanding the local reactivity in polar organic reactions through electrophilic and nucleophilic Parr functions. *RSC Adv.* 3: 1486-1494.